JOURNAL OF SOLID STATE CHEMISTRY 115, 532–539 (1995)

Ultrasound Effects on Various Oxides and Ceramics: Macro- and Microscopic Analyses

M. Gasgnier, L. Albert, J. Derouet, and L. Beaury

ER209, CNRS Bellevue, 1 Pce. A. Briand, 92195 Meudon Cedex, France

Received February 16, 1994; in revised form July 25, 1994; accepted July 28, 1994

The sonochemistry of a heterogeneous medium such as a liquid/solid powder has been studied for various oxides (lead, manganese, aluminum, rare earth elements, silicon, titanium, and chromium) and ceramics (superconductor and titanium–yttrium compounds). The chemical transformations that occur during ultrasound treatments appear to differ from one material to another. The most important results relate the leaching of Pb_3O_4 which forms the dioxide in dilute acetic acid; and the formation of α-Al_2O_3, and $Al(OH)_3$ from the η-Al_2O_3 form. It has been established that ultrasound treatments decrease the grain size and smooth small particles. © 1995 Academic Press, Inc.

INTRODUCTION

In a former article (see Ref. 1) it was shown that ultrasound (US) irradiations quicken the selective dissolution of rare earth (R) higher oxides (Pr_6O_{11} and Tb_4O_7 respectively) to form the dioxides (RO_2). In this paper the same procedure has been used to study the possibility of phase transitions, and to control the grain size distribution of various oxides and ceramics. The phenomena which govern the so-called sonochemistry properties were previously described in terms of cavitation (collapse of bubbles) and shock-waves. However, besides implosion of bubbles, it has been recently observed that in the final phase the bubbles might also be fragmented into microbubbles. That could induce charge accumulation at the bubble–liquid interface and locally intense electric fields (2). Therefore the extreme conditions which take place during collapse and fragmentation should also be associated with plasma (or corona-like) chemistry (3). As a consequence the phenomena which occur in a pure liquid are as yet, at present, very difficult to explain clearly. They become still more complex to resolve in the case of a liquid/solid medium. For example, one can ask questions such as: What is the prevailing phenomenon which occurs at a triple interface such as liquid/solid/bubble? Is it possible that gas microbubbles trapped close to the surface of a solid particle may collapse? In the case of a dominant electric field phenomenon, how will metallic or insulating particles react at their surfaces? Up to now no one experiment has been carried out in this field of research. The aim of this paper is to show how US irradiations can change, or not change, the crystalline characteristics (new crystallographic phases, grain size distribution, ...) of various materials such as pure, binary, or ternary oxides.

EXPERIMENTAL

The experiments were carried out with an US generator (Branson apparatus, 20 kHz) (1). Compared to the first series of experiments, the main improvement to the method was, in some cases, the use of a double-walled glass-vessel, that permits maintainance of a continuous flow of cool water between the walls. Such an apparatus affords three advantages. First, it avoids heating of the liquid (water, dilute acids, dodecane) inside the glass vessel. Second, it diminishes the evaporation of part of the dilute acids. Third, it allows increasing the output power of the generator. Moreover, the choice of the liquid was made as a function of the material. For example, the superconductor ceramics ($YBa_2Cu_3O_x$) were dipped into neutral liquids such as dodecane to avoid reaction with oxygen or OH radicals from water dissociation (1). On the other hand, it has been pointed out that the metallic horn might be attacked in two different ways. The first is abrasion due to hard particles when they move rapidly along the horn. The second is an acidic attack on the envelope. After sonication (10 hr) of a 5% acetic acid solution (200 ml) one can sometimes observe a black deposit of metallic particles at the bottom of the glass-vessel. After it was separated from the liquid, energy dispersive X-ray analyses revealed the presence of titanium (98%) and traces (2%) of Fe, Mo, and Y. Moreover, the X-ray diffraction patterns show that the diffraction lines refer to the hexagonal structure of the titanium. The oxide and ceramic materials were characterized before and after treatment by X-ray diffraction, scanning electron microscopy (SEM), transmission electron microscopy (TEM), energy dispersive X-ray spectroscopy (EDX), and granulometry.

0022-4596/95 $6.00

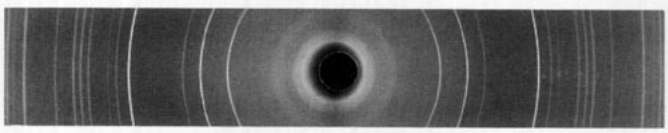

FIG. 1. XDP of the pure PbO_2 compound.

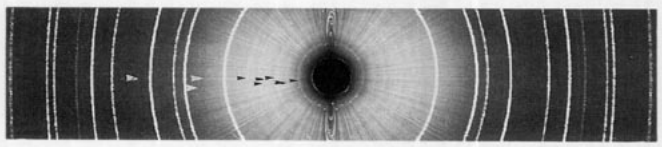

FIG. 2. XDP showing the coexistence of the α-Al_2O_3 phase and of an unknown compound the X-ray lines of which are indicated by black and white arrows.

RESULTS

The Orthoplumbate as Pb_3O_4

Heterogeneous valence state solids are very exciting materials in the sense that the different metallic ions can be separated to prepare other solid phases. Such a phenomenon has been reported and discussed for higher praseodymium and terbium oxides (1, 4–8), Pb_3O_4 (9, 10) and Mn_3O_4 (11). Generally the "solvolytic disproportionation," or leaching, or selective dissolution, occurs in the course of the reaction of solids dipped into various acids. In the case of Pr_6O_{11}, a 5% dilute acetic acid solution permits removal of the Pr^{3+} ions from the solid, whereas the Pr^{4+} ones remain in a solid residue as PrO_2.

For the intermediate Pb_3O_4 oxide, it is possible that a 5% dilute acetic acid solution may be able to generate the following reaction:

$$Pb_3O_4 + 4H^+ \rightarrow PbO_2 \downarrow + 2Pb^{2+} + 2H_2O.$$

In this way 7.9 g of red lead oxide (minium, primitive tetragonal cell) was dipped into a 5% acetic acid solution (200 ml) contained in a double-walled glass vessel. The mixture was subjected to US (output power about 175 W) for 45 min, after which the red solid became brown. Moreover, the small particles appeared to form a colloid-like suspension, which was separated from the liquid by centrifugation. A weight balance showed that 2/3 of the Pb_3O_4 was dissolved according to the stoichiometric reaction. X-ray diffraction patterns (XDP) revealed that all the X-ray lines corresponded to those of PbO_2 (primitive tetragonal cell) (Fig. 1). It appears therefore that US treatments quicken the obtaining of the lead dioxide. That makes it possible to avoid using either dilute boiling nitric acid or concentrated boiling acetic acid, as generally reported necessary to generate this reaction.

The Orthomanganate as γ-Mn_3O_4

An initial red-brown powder was characterized by XDP according to the centered tetragonal cell of the γ-Mn_3O_4 compound. To attempt to form the MnO_2 compound three different experiments were carried out. For the first one, 4.18 g of γ-Mn_3O_4 was dipped into a 5% dilute acetic acid solution (200 ml). After sonication (2 hr, output power about 200 W) the powder turns totally brown. Surprisingly, XDP reveals the formation neither of manganese dioxide, nor of another oxide. On the other hand, the classical chemical reaction for γ-Mn_3O_4 leaching is reported to be carried out in nitric acid. But it is not possible to dip the metallic horn into this acid without damage. Under these conditions, formic acid has tentatively been used. The second set of experiments was to dip 2.8 g of γ-Mn_3O_4 into a pure formic acid bath. After sonication (2 hr, output power about 175 W) the particles became brown and formed a colloid-like suspension in the liquid. After addition of distilled water, which should allow a better separation of the constituents, a total and rapid dissolution of the solid phase was possible. It is likely that partial hydrolysis of the powder occurs during sonication. This reaction should be due to decomposition of the formic acid to form H_2O and CO. The third procedure for forming manganese dioxide was carried out by dipping 2.85 g of γ-Mn_3O_4 into 5% dilute formic acid. The mixture was sonicated (output power about 175 W) for about 6 hr. After the powder was dried, XRD revealed the coexistence of three compounds. The first one, which is the most important, was hydrated manganese formate $(COOH)_2Mn \cdot 2H_2O$ (12), of which all the X-ray lines of the monoclinic structure can be indexed. Moreover, the lines on the pattern are dotted, indicating the formation of large crystals. One must remember that in the case of the praseodymium oxide a mixture such as formic acid + acetic acid led to the formation of praseodymium formate (1). The second compound was manganese monoxide (13), of which the more intense diffraction lines of the cubic structure (such as (200)) is indexed. The third

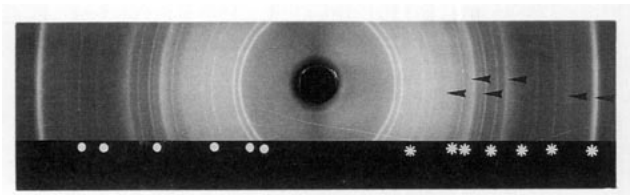

FIG. 3. XDP exhibiting the coexistence of three compounds, η-Al_2O_3 (arrows), α-Al_2O_3 (asterisks), and $Al(OH)_3$ (full circles).

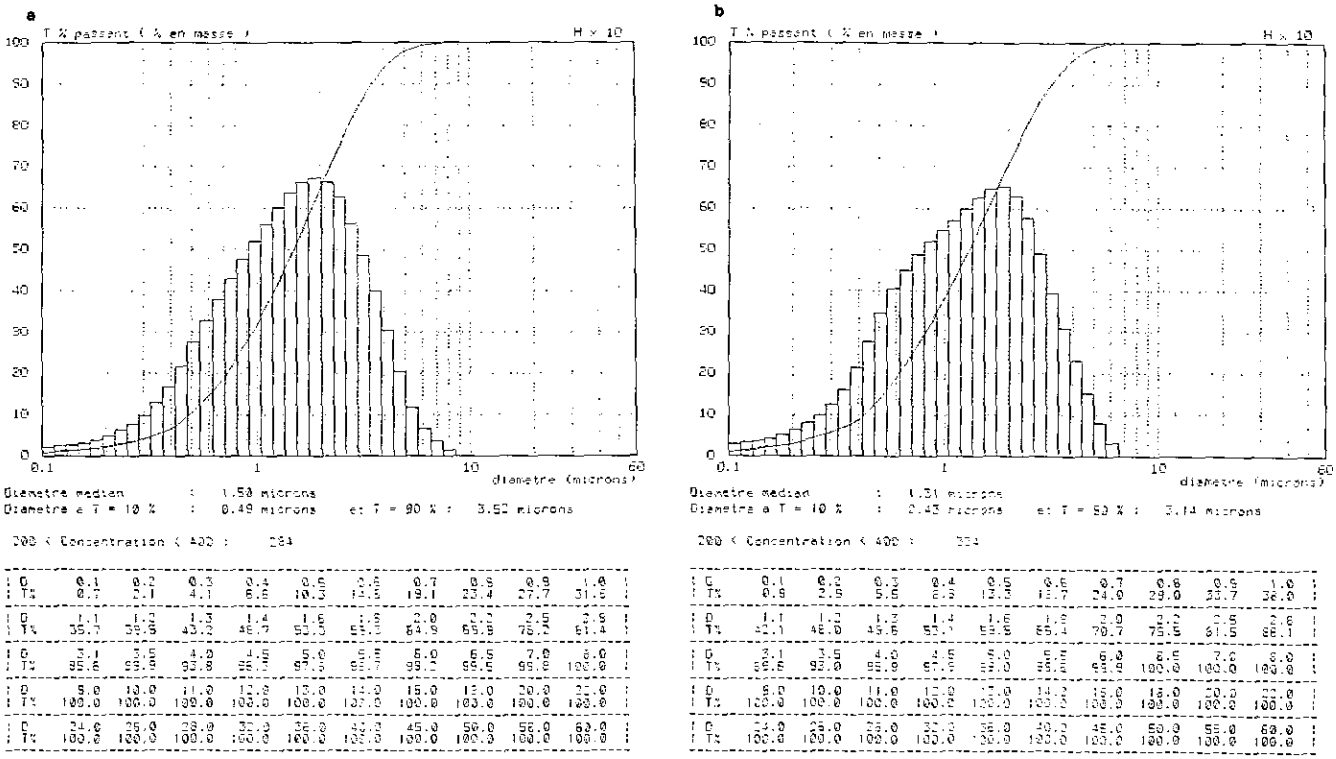

FIG. 4. Grain size distribution of a Dy_2O_3 powder in water: (a) initial material; (b) after US treatment (3 hr).

compound was γ-Mn_3O_4, of which the two intense lines (211) and (200) are observed on the pattern.

The Aluminum Oxides and Hydroxide

A commercial alumina (Merck) was used as the initial material. XDP revealed that the coarse white powder crystallized according to the spinel cubic lattice ($a = 0.795$ nm) of the η-Al_2O_3 form of the aluminas (14). To study US effects two sets of experiments were carried out.

In the first case, the powder was dipped into distilled water. The mixture was put into a double-walled glass vessel and sonicated for 140 min (output power about 160 W). During a first treatment the powder became grey due to appreciable abrasion of the horn. EDX analyses revealed that alumina particles contained small amounts of titanium. On the other hand, XDP showed that two different line systems might be indexed (Fig. 2). The first was for the α-Al_2O_3 form of alumina (corundum, with a rhombohedral lattice), and the second was possibly for an orthorhombic structure ($a = 1.140$, $b = 1.040$, $c = 0.835$ nm), but it corresponds neither to a known alumina phase, nor to a binary aluminum–titanium oxide. In the

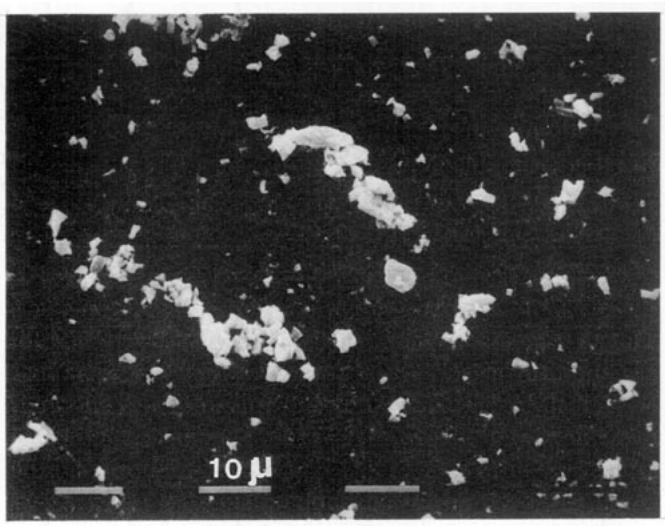

FIG. 5. SEM micrography of Dy_2O_3 particles (×1850). Small aggregates can be observed.

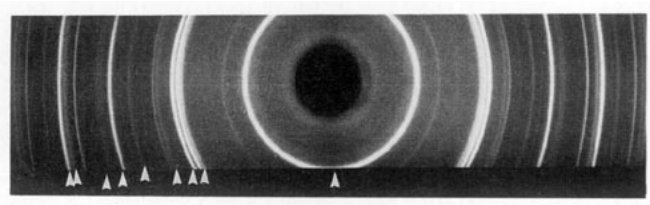

FIG. 6. XDP showing the coexistence of the $Y(OH)_3$ and C-Y_2O_3 phases. The diffraction lines of $Y(OH)_3$ are indicated by arrows.

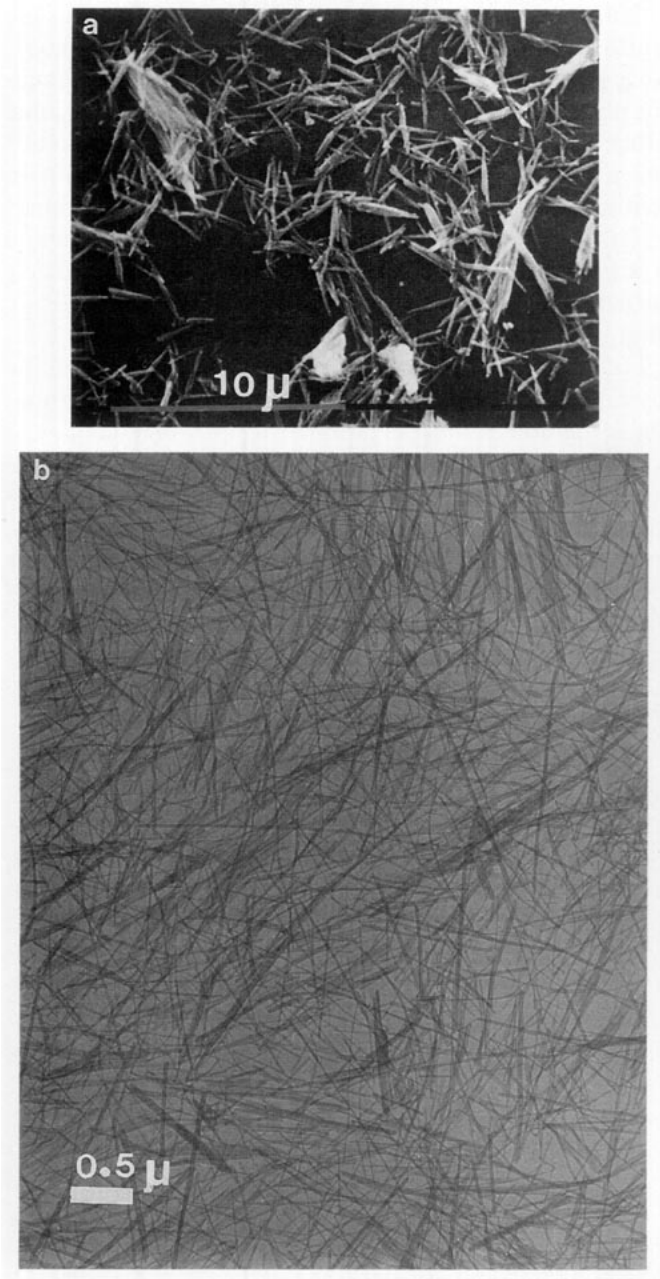

FIG. 7. SEM images characteristic of the $Y(OH)_3$ compound: (a) needle-like crystallites (15 days after the US treatment) (×5000); (b) hair-like crystallites (3 months after the sonication experiment) (×50,000).

course of a second set of experiments the horn was not abraded (EDX analyses did not reveal the presence of titanium). XDP showed the coexistence of three different line systems (Fig. 3). Two of them are for the η-Al_2O_3 and α-Al_2O_3 forms of alumina, and the third for the hydroxide $Al(OH)_3$ (Bayerite form, with a monoclinic cell (15)).

The second set of experiments was carried out in a neutral liquid, dodecane, instead of water. During sonication (8 hr, output power about 230 W) the horn was not attacked, as revealed by EDX analyses. In this case, XDP showed that only the η- and α-Al_2O_3 phases coexisted. TEM observation of the crushed powders showed very intricate electron diffraction patterns. One can only indicate that at the mesoscopic scale other alumina phases are formed. The great complexity of the patterns has not allowed the determination of these structures, which cannot be attributed to the classical structures.

The Rare Earth Sesquioxides

Five rare earth sesquioxides (R_2O_3, R = Y, Eu, Gd, Dy, and Ho) powders were irradiated for periods of 3–7 hr. XDP did not reveal phase transitions such as C-R_2O_3 (cubic centered) → B-R_2O_3 (monoclinic) (16, 17). Particle size distribution (Granulometer CILAS : HR850) measurements and TEM observations were performed for Dy_2O_3 and Y_2O_3.

(a) EDX analyses permit detection of the presence of other R oxides (R = Ce, Pr, and Tb) as impurities in the Dy_2O_3 powders. The grain size distribution shows that the average diameter of the particles was 1.50 μm before irradiation and 1.31 μm after US treatment (3 hr) (Figs. 4a and 4b). Moreover, comparison of the two curves reveals that a higher density of small crystallites is formed after sonication: the percent ratio of grains with a size of 1.00 μm increases from 32 to 38%. This has been backed up by SEM observations, where grains of about 0.3 μm long were visualized (Fig. 5). A part of the liquid/solid solution was poured into a bottle and set aside for 5 months. After this period it was observed that the major part of the grains remained suspended in the water. The mixture was a sol–gel-like material. It was also observed that the larger particles were deposited at the bottom of the glass-vessel.

(b) Another experiment was carried out with a coarse Y_2O_3 powder. The average size of the crystallites was

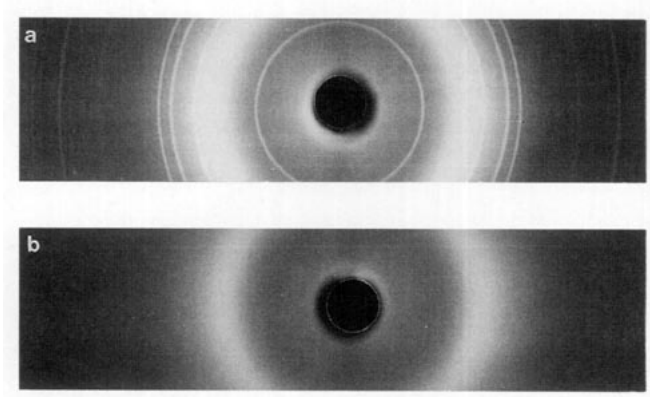

FIG. 8. XDP relative to a SiO_x compound: (a) coexistence of an amorphous compound and of an unknown crystalline phase; (b) fully amorphous powder after sonication.

close to 8.30 μm, and a large part of them had a size between 10 and 25 μm. After sonication (5 hr) the median diameter decreased to 6.90 μm. The size of the major part of the grains was between 5 and 20 μm. This experiment was carried out in a broadly dilute acetic acid solution (≈2% in water). Surprisingly, XDP revealed the formation of the trihydroxide ($Y(OH)_3$) in coexistence with the C-Y_2O_3 compound (Fig. 6). Just after treatment, SEM observations permitted visualization of needle-like crystals in coexistence with some scattered crystals (Fig. 7a). After a longer period (3 months), the crystallites remained suspended in the solution. TEM experiments permitted observation of long hairlike crystallites (Fig. 7b) which were longer than those observed for the freshly irradiated powder. A part of the aging sample was dried, and XDP revealed that the C-Y_2O_3 → $Y(OH)_3$ transition was achieved. In general heavy R trihydroxides are prepared from R_2O_3 compounds by hydrothermal growth in a NaOH mineralizer that sustains high pressures and temperatures of 500–670 K for several days (18–20). Moreover, the possibility of small amounts of Na inside the needle crystals cannot be excluded. The use of this procedure can be avoided by means of US treatments. In our case dilute acetic acid could play the role of catalyst. One must recall that for light R the formation of the hydroxide is easier, either by immersion in distilled water at 373 K (21), or in the course of the formation of the oxide from metallic thin films (22).

The Silicon Oxides

Five different SiO_x powders, immersed in water, were irradiated for 7 hr. Two of them, initially amorphous, did not undergo transformations. The third one, SiO_2 α-tridymite, remained crystallized after US treatments. The fourth sample (Lichlorosorb 80) was initially amorphous. After sonication, XDP revealed the formation of a crystalline phase. From the five weak diffraction lines, two cubic lattices can be indexed: one as fcc (a_F = 0.540 ± 0.003 nm) and the other as bcc (a_1 = 0.763 ± 0.003 nm). In contrast, the fifth specimen (Silica gel, Prolabo) was characterized by the coexistence of an amorphous phase and of an unknown crystallized silica form (Fig. 8a). After further US irradiation the powder became completely amorphous (Fig. 8b).

The last two results are difficult to interpret. Indeed, the cavitation effects should act oppositely during irradiation: The formation of small crystallites (fourth sample) should be induced by high temperature and high pressure conditions. This behavior can be associated with that of amorphous thin films annealed by means of the electron beam inside a TEM (23–25). In an opposite manner, microjets and shock waves can destroy an unstable compound and allow creation of conditions inducing a crystalline → amorphous transformation.

The Superconducting YBaCuO Ceramic

$YBa_2Cu_3O_z$ powders (Rhône-Poulenc products) were irradiated for 7 hr in dodecane. Before and after US treatments, XDP and EDP revealed small amounts of the Y_2BaCuO_5 phase and of the $BaCuO_2$ compound within the matrix. Grain size distribution analyses (Horiba L 900 apparatus) show that the starting sample is characterized by only one kind of grain (Fig. 9a), with a median diameter of 3.585 μm and a specific surface of 19,306 cm^2cm^{-3}. After sonication, the curve (Fig. 9b) exhibits two maxima at 1.80 μm and 4.00 μm. The average diameter is

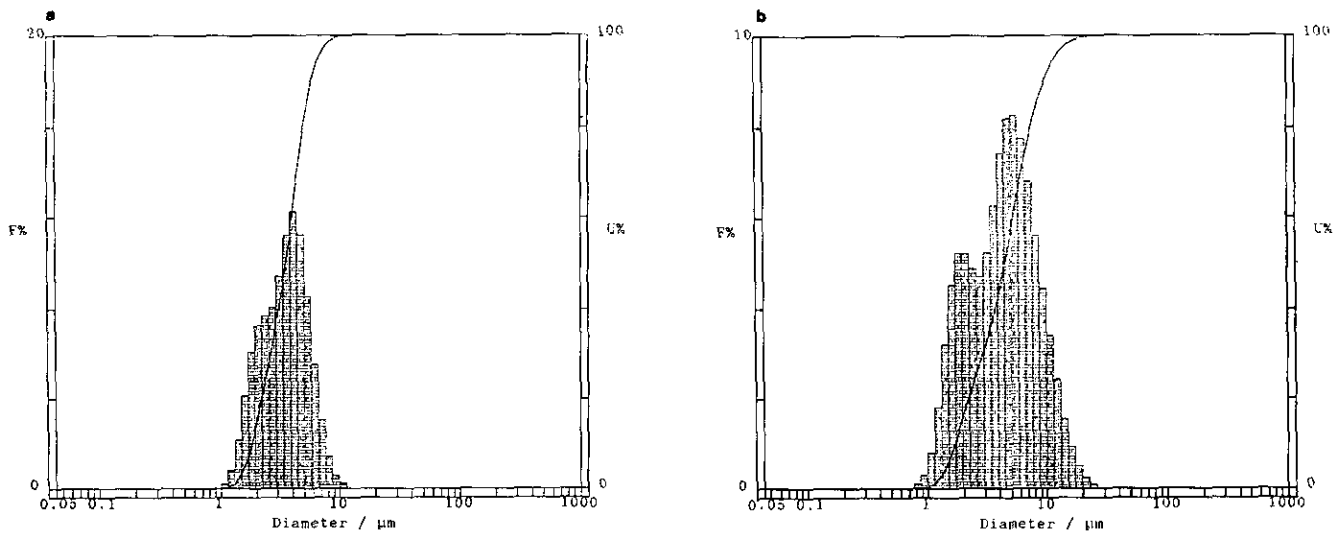

FIG. 9. Grain size distribution of a $YBa_2Cu_3O_z$ powder: (a) starting material; (b) irradiated sample (7 hr).

4.492 μm and the specific surface is 17,491 cm^2cm^{-3}. TEM observations show that the starting powder is composed grains characterized by holes and spikes (Fig. 10a). After US irradiation these configurations disappear, and the crystallites become denser and smoother (Fig. 10b). In addition, one can visualize aggregates composed of grains of different sizes (Fig. 10c). This observation is in good agreement with the grain size distribution (Fig. 9b).

After sonication, part of the powder was slightly compressed, without thermal treatment, to form a pellet in order to record some magnetic properties. First, as a function of the temperature and under an applied field of 2 KOe, the onset of the decrease of the magnetic moment occurs at 92.5–93 K, in good agreement with the best values reported for the $YBa_2Cu_3O_{7-x}$ ceramics. Second, hysteresis cycles, at 4.2 K, and under an applied magnetic field of 3.5 KOe, reveal that the magnetic moment decreases to a minimum value of −0.24 emu. These results show that the superconducting properties of this powder are preserved after sonication.

The Titanium–Yttrium Oxide Ceramic

To form the $Y(OH)_3$ compound, Y_2O_3 powder was dipped into 3% dilute acetic acid. But, in some cases, after US treatment a grey deposit was observed at the bottom of the glass vessel. The dried powder consisted of three main components, Ti metal, Y_2O_3 (centered cubic form), and another compound, as revealed by XDP (Fig. 11). Indexation of the diffraction lines, which did not correspond either to Ti, or to Y_2O_3, leads to the conclusion, as a first approximation, that the third component should be the monoclinic phase of Y_2TiO_5 (a = 1.549,

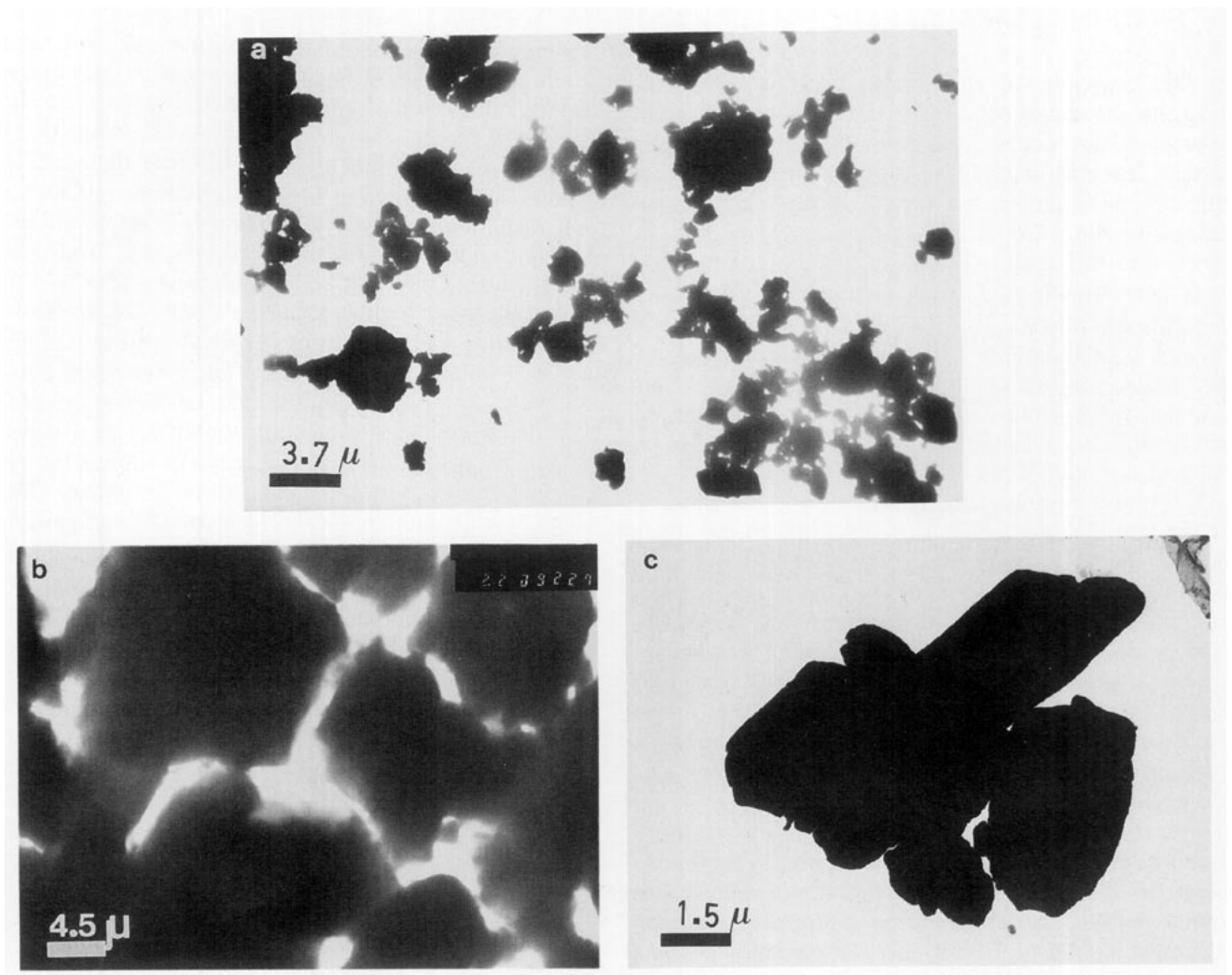

FIG. 10. TEM images of the $YBa_2Cu_3O_z$ ceramic: (a) starting powder, in which the grains present numerous holes and spikes (×2700); (b) and (c) aspect of the particles after US treatments (×2200 and ×7000, respectively).

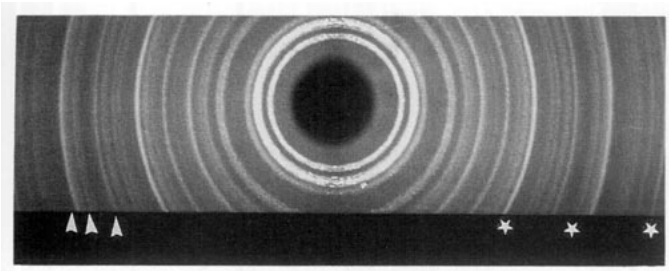

FIG. 11. XDP showing the coexistence of Ti metal (white arrows, characteristic of the hexagonal system, such as a triplet), C-Y_2O_3 (asterisks), and possibly Y_2TiO_5 compound (other diffraction lines, except the first intense one which cannot be indexed by means of the characteristic monoclinic system).

$b = 0.5252$, $c = 0.1528$ nm, and $\beta = 87°65$) (26). However, since some other lines were not indexed, it is possible that a fourth compound was formed during sonication.

CONCLUSION

It has been shown that during US treatments of heterogeneous liquid/solid mixtures (powders) different phenomena may occur. One of the most interesting is the rapid leaching of Pb_3O_4 to form PbO_2 in a 5% dilute acetic acid solution. Such a result can be linked to that obtained in the case of higher rare earth oxides (1). However, it is difficult to establish a general law because it was not possible to form manganese dioxide under the same conditions. This can be discussed, first, in terms of crystallographic structures. Indeed, the two initial oxides do not crystallize according to the same tetragonal space group, and their lattice parameters are entirely different. Thus, the acid attack on γ-Mn_3O_4 (centered tetragonal) should be less easy than that on Pb_3O_4 (primitive tetragonal). However, one can observe that the two dioxides crystallize according to the space group of the TiO_2 rutile form. The second hypothesis should be linked to the toughness of the crystals. Last, one can discuss the reactivities in terms of the acidity of the oxides. Indeed, γ-Mn_3O_4 and Pb_3O_4, are known as saline oxides, and, of course, can be reduced or oxidized, according to the reactive medium. So, in the case of a strong acid, such as the formic acid, manganese monoxide is formed. One must add that the dioxides have an amphoteric character.

The second important result to be discussed relates to obtaining the alumina corundum. Generally, as previously reported (27), the crystalline transitions of the various alumina phases occur at high temperature. For example, in the case of η-Al_2O_3 transitions occur such as

$$\eta\text{-}Al_2O_3 \xrightarrow[1200\ K]{} \theta\text{-}Al_2O_3 \xrightarrow[1500\ K]{} \alpha\text{-}Al_2O_3.$$

It is also interesting to notice that the formation of the $Al(OH)_3$ bayerite form from the η-Al_2O_3 phase is not a conventional chemical reaction (12, 25). In the same way, the formation of the $Y(OH)_3$ compound from Y_2O_3 dipped into a very dilute acetic acid solution appears very surprising. Indeed, in general C-Y_2O_3 is highly stable and can only form the hydroxide through special experimental procedures. Last, the formation of binary titanium–yttrium oxides seems also far from the conventional chemical reactions. The addition of very fine metallic particles to a fine oxide powder could induce chemical reactivities not expected in the bulk by means of US treatments.

However, some experiments were not successful. It was not possible to observe the C-$R_2O_3 \rightarrow$ B-R_2O_3 transition after sonication of the cubic sesquioxides. Likewise, other experiments did not allow formation of R_2O_2S after sonication of mixtures such as C-R_2O_3 (R = La or Y)/ either sulfur (powder), or thiosulfate (liquid). In the same way, it was not possible to form CrO_2 through the following experiments: first, addition of a Cr_2O_3 powder to a 10% dilute $HClO_4$ solution (in a test tube); second, mixing of Cr_2O_3 and CrO_3 in water. Last, another attempt was carried out to study the possibility of observing the phase transitions of the titanium dioxides. After sonication for long periods (8 to 18 hr) of four different samples, TiO_2 (anatase), TiO_2 (rutile), TiO_2 (amorphous), and TiO_2 (anatase + rutile), no transition phase was detected either by XDP or by TEM. To verify these results, new experiments will be carried out with higher output powers.

Many of the experiments carried out by US irradiations have opened a new route for chemical syntheses. In particular, leaching reactions are often accelerated by this treatment. However, it appears that the phenomena which occur in the course of sonication are not yet clearly established. One can only assert that the cavitation of bubbles, the generation of shock waves, and the secondary effects which result from them involve the breaking of particles. These effects should be more suited to reactions in acidic solutions. On the other hand, US treatments appear to be a powerful procedure for obtaining very small grains (more than submicrometric in some cases); and it should be possible to obtain nanometric particles after long sonication periods and with higher output powers.

ACKNOWLEDGMENTS

The authors are indebted to Dr. P. Tremblay (Laboratoire des Sciences de la Terre, Université Paris-Sud, Orsay, France) for performing the EDX and SEM experiments.

REFERENCES

1. M. Gasgnier, L. Albert, J. Derouet, L. Beaury, P. Maestro, T. Chopin, and P. Caro, *J. Solid State Chem.* **112,** 367 (1994).
2. N. Voglet, F. Mullie, and T. Lepoint, *New J. Chem.* **17,** 519 (1993).

3. T. Lepoint, F. Mullic, N. Voglet, D. N. Yang, J. Vandercammen, and J. Reisse, *Tetrahedron Lett.* **33,** 1015 (1992).
4. A. F. Clifford, *in* "Rare Earth Research II" (K. S. Vorres, Ed.), pp. 45–50. Gordon & Breach, New York, 1964.
5. Z. C. Kang and L. Eyring, *J. Solid State Chem.* **75,** 52 (1988).
6. M. Gasgnier, G. Schiffmacher, L. Albert, P. Caro, H. Dexpert, J. M. Esteva, C. Blancard, and R. Karnatak, *J. Less-Common Met.* **156,** 59 (1989).
7. G. Brauer and B. Pfeiffer, *J. Less-Common Met.* **5,** 171 (1963).
8. Z. C. Kang and L. Eyring, *J. Solid State Chem.* **75,** 60 (1988).
9. C. Bruckner, *Chem. Z.* **51,** 55 (1927).
10. Z. C. Kang, L. Machesky, H. A. Eick, and L. Eyring, *J. Solid State Chem.* **75,** 73 (1988).
11. D. R. Giovanoli, W. Feitknecht, R. Maurer, and H. Hani, *Chimia* **30,** 307 (1976).
12. JPCDS-ICDD Card No. 18-823.
13. JPCDS-ICDD Card No. 7-230.
14. J. W. Newcombe, H. W. Heiser, A. S. Russell, and H. C. Stumpf, ALCOA Technical Paper No. 10 (second revision), pp. 1–88. ALCOA, Pittsburgh, 1960.
15. JCDS-ICDD Card No. 20-11.
16. M. Gasgnier, *Phys. Status Solidi A* **57,** 11 (1980).
17. C. Boulesteix, *Phys. Status Solidi A* **86,** 11 (1984).
18. S. Mroczkowski, J. Eckert, H. Meissner, and J. C. Doran, *J. Cryst. Growth* **7,** 333 (1970).
19. S. Mroczkowski and J. Eckert, *J. Cryst. Growth* **13/14,** 549 (1972).
20. P. V. Klevtsev and L. P. Sheina, *Inorg. Mat.* **1,** 838 (1965).
21. M. Gasgnier, G. Schiffmacher, L. Albert, P. Caro, H. Dexpert, J. M. Esteva, C. Blancard, and R. C. Karnatak, *J. Less-Common Met.* **156,** 59 (1989).
22. M. Gasgnier, *Phys. Status Solidi A* **57,** 11 (1980).
23. M. Gasgnier, G. Schiffmacher, D. Svoronos, and P. Caro, *J. Microsc. Spectrosc. Electron.* **13,** 13 (1988).
24. M. Gasgnier, G. Shiffmacher, and P. Caro, *J. Less-Common Metals* **50,** 177 (1976).
25. M. Gasgnier, F. Lagnel, B. Poumellec, and J. F. Marucco, *Thin Solid Films* **187,** 25 (1990).
26. F. Queyroux, A. Harari, and R. Collongues, *Bull. Soc. Fr. Ceram.* **36,** 72 (1966).
27. H. C. Stumpf, A. S. Russell, J. W. Newcombe, and C. M. Tucker, *Ind. Eng. Chem.* **42,** 1398 (1950).